

Dust in the wheel: The Cartwheel galaxy in the Mid-IR^{*}

V. Charmandaris^{1,2}, O. Laurent², I.F. Mirabel², P. Gallais², M. Sauvage², L. Vigroux², C. Cesarsky², and P.N. Appleton³

¹ Observatoire de Paris, DEMIRM, 61 Av. de l'Observatoire, F-75014 Paris, France

² Service d'Astrophysique, CEA-Saclay, F-91191 Gif-sur-Yvette Cedex, France

³ Department of Physics and Astronomy, Iowa State University, Ames, IA 50011, USA

Received 9 July 1998 / Accepted 13 October 1998

Abstract. We present mid-infrared images at $6.7\ \mu\text{m}$ and $15\ \mu\text{m}$ of “The Cartwheel” (AM 0035-33), the prototypical collisional ring galaxy. The observations, taken with ISOCAM, reveal the distribution of hot dust in the galaxy and its two companions in the north-east. The intensity of the Mid-IR emission from the outer star forming ring of the Cartwheel shows considerable azimuthal variation and peaks at the most active $\text{H}\alpha$ region of the ring. The $15\ \mu\text{m}$ to $6.7\ \mu\text{m}$ flux ratio of 5.2 is the highest among all the galaxies of our sample. A surprising result of our observations is the discovery of significant emission from the inner regions of the galaxy, including the inner ring, spokes and nucleus, where previously only low level $\text{H}\alpha$ emission had been reported. At $6.7\ \mu\text{m}$, this emission is stronger than the one from the outer star forming ring, and at $15\ \mu\text{m}$, it represents 40% of the emission from the outer ring. The $\text{H}\alpha$ to Mid-IR flux ratios from the inner regions are consistent with the heating of grains from weak star formation activity.

Key words: infrared: ISM: continuum – galaxies: starburst – galaxies: interactions – galaxies: individual: The Cartwheel – stars: formation

1. Introduction

Collisional ring galaxies, of which the Cartwheel is the “prototypical” candidate, are believed to form when an “intruder” galaxy passes through the center of a rotating disk of a larger “target” galaxy (Lynds & Toomre 1976; Theys & Spiegel 1976; Appleton & Struck-Marcell 1996 and references therein). The perturbation triggers a radially expanding ring-like density wave on the disk, causing massive star formation in the ring (see Appleton & Marston 1997). The symmetry and well defined dynamical history of ring galaxies has made them ideal candidates for studies of the phase transition of the interstellar medium due to collisionally induced star formation.

Send offprint requests to: V. Charmandaris
(v.charmandaris@obspm.fr)

^{*} Based on observations with ISO, an ESA project with instruments funded by ESA Member States (especially the PI countries: France, Germany, the Netherlands and the United Kingdom) with the participation of ISAS and NASA.

The Cartwheel galaxy was discovered by Zwicky (1941) at a distance of 121 Mpc ($H_0=75\ \text{km s}^{-1}\ \text{Mpc}^{-1}$). It has a bright outer ring and an inner ring which is connected to the outer one with a series of spokes (see Higdon 1996 Fig. 1). Three small companion galaxies located north and north-east of the ring complete the group. It is still unclear which of the companions is the culprit for the creation of the Cartwheel ring (Davies & Morton 1982; Struck-Marcel & Higdon 1993), but it is likely that each of them contains sufficient mass to trigger the generation of the star forming ring (see discussion by Appleton & Struck-Marcell 1996). On-going efforts to simulate the dynamics of the system have been focused on the nearby companion G2 (Bosma priv. comm.) and on the most distant one, G3, (Struck 1997; Horellou priv. comm.) which seems to be connected to the Cartwheel with a plume of H I gas (Higdon 1996).

Due to its unique morphology, the Cartwheel has been the subject of early optical studies (Theys & Spiegel 1976; Fosbury & Hawarden 1977) as well as dynamical modeling (Struck-Marcel & Higdon 1993; Hernquist & Weil 1993). The outer ring of the Cartwheel ($\sim 70''$ in diameter) is expanding, has blue colours and is populated by massive star-forming regions (Higdon 1995, Amram et al. 1998). Most of the star formation though, appears to occur in a localized area of a few H II complexes in the southern sector of the ring. The $\text{H}\alpha$ emission, as well as the 20cm and 6cm radio continuum emission vary as a function of the azimuth along the ring and peak in the same region of the southern sector (Higdon 1996). Optical and near-IR imaging show strong radial colour gradients in the disk behind the outer ring, which may trace the evolution of the stellar population in the wake of the density wave (Marcum et al. 1992). Broad band images obtained with the HST (Borne et al. 1997; Appleton 1998) reveal in unprecedented detail the distribution of massive young clusters around the outer ring, as well as the diffuse and knotty structure of the so called “spokes”.

The inner ring ($\sim 18''$ in diameter) and nucleus of the Cartwheel seem gas-poor, have very little H I (Higdon 1996), and no CO emission has been detected so far (Horellou et al. 1995). The failure to detect molecules from the galaxy may be a matter of sensitivity, or low metallicity since recent $\text{H}\alpha$ observations (Amram et al. 1998) indicate that there is some low-level star formation in the central regions. Furthermore, HST observations clearly show the presence of well defined dust lanes,

Table 1. Observational parameters

Name:	The Cartwheel	
Coordinates:	a(J2000)	00 ^h 37 ^m 41.62 ^s
	δ(J2000)	-33° 43′ 00.4″
Observations:	Instrument	ISOCAM
	Date	November 23, 1996
	Field of view	4.2 × 4.2 arcmin
	Pixel size	6″
Filters:	6.75 μm (LW2)	range: [5–8.5] μm
	15 μm (LW3)	range: [12–18] μm
Exposure times:	Number of frames	141 per filter
	Frame exposure time	2.1 s
	Total LW2 exposure	5 min
	Total LW3 exposure	5 min

as well as some interesting compact blue comet-like regions on and near the inner ring (Struck et al. 1996). The heads of the cometary structures were suggested to be regions of star formation triggered by the passage of dense clouds moving supersonically through the inner-ring gas. Such clouds may result from infall from the H I plume, or cloud-cloud collisions in the disk.

Although the galaxy as a whole was detected by IRAS at longer wavelengths (Appleton & Struck-Marcell 1987), our ISOCAM Mid-IR observations represent the first detection and mapping of the distribution of the hot dust throughout the galaxy and its nearby companions.

2. Observations and data reduction

The Cartwheel group was observed with ISOCAM (Cesarsky et al. 1996) on November 23 1996 (ISO revolution 372). It was part of the ISO (Kessler et al. 1996) guaranteed time program CAMACTIV (PI. I.F. Mirabel) which prime goal was the Mid-IR imaging of more than 20 nearby active/interacting galaxies. Two broad band filters centered at 6.75 μm (LW2), and 15 μm (LW3), with a lens resulting in a 6″ pixel field of view, were used to create a 2 × 2 raster map. The Mid-IR maps cover the Cartwheel galaxy and the two nearby companions G1 and G2. More details on the observational parameters are presented in Table 1.

The standard data reduction procedures described in the ISOCAM¹ manual were followed (Delaney 1997). Dark subtraction was performed using a model of the secular evolution of ISOCAM’s dark current (Biviano et al. 1997). Cosmic rays were removed using a multi-resolution median filtering method (Starck et al. 1996) while the memory effects of the detector were corrected using the so-called IAS transient correction algorithm which is based on an inversion method (Abergel et al. 1996). The final raster was constructed after using the instru-

¹ The ISOCAM data presented in this paper were analyzed using “CIA”, a joint development by the ESA Astrophysics Division and the ISOCAM Consortium led by the ISOCAM PI, C. Cesarsky, Direction de Sciences de la Matière, C.E.A., France.

mental flat fields and correcting for the lens field distortion. These methods and their consequences are discussed in detail in Starck et al. (1998).

The ISOCAM LW2 filter mainly samples Mid-IR flux originating from the Unidentified Infrared Bands (UIBs), centered at 6.2, and 7.7 μm. This feature emission is attributed to stretching modes of 2-dimensional molecules (often called polycyclic aromatic hydrocarbons, or PAHs) having C–C and C–H bonds. It may also contain some contribution from the long wavelength blackbody tail of the stellar photospheric emission. The LW3 filter though, is almost two times wider than the LW2 and it is principally sensitive to the presence of the thermal continuum emission of very small grains. Regions of massive young stars can heat very efficiently the surrounding dust grains and create a strong thermal Mid-IR continuum (i.e. Vigroux et al. 1996). This continuum appears at 12 μm, its slope steepens as the intensity of the ionizing field increases, and it dominates the Mid-IR emission up to 18 μm (the long wavelength detection limit of ISOCAM). Several forbidden lines and few UIBs may also appear in the wavelength range covered by LW3, but their contribution to the total flux is usually negligible when the thermal continuum is present.

3. The morphology of the Mid-IR emission

As one can observe from Fig. 1, despite of not being detected in the IRAS 12 μm and 25 μm bands (upper limits of ~0.1 Jy in both bands), there is Mid-IR emission from the Cartwheel group (see Table 2) and it displays an interesting spatial distribution. In the following subsections, we discuss the morphology and nature of the Mid-IR emission from the two companions, the outer star forming ring of the Cartwheel, as well as from the central regions of the ring galaxy.

3.1. The companions

The morphological types of the two nearby companions of the Cartwheel are distinctly different. The eastern companion (G2) is an early type S0 galaxy. No H I is directly associated with this galaxy (Higdon 1996) and no star formation activity has been detected (Amram et al. 1998). On the contrary, the western companion (G1), a late type galaxy with somewhat irregular spiral arms, has $2.7 \times 10^9 M_{\odot}$ of H I and emits strongly in H α , which indicates the presence of a young stellar population (see Fig. 1 of Amram et al. 1998). The LW2 fluxes of the two galaxies, presented in Table 2, are weak but very similar. This is not true though for the LW3 emission where only the western companion (G1), is detected.

This contrast on the LW2 over LW3 emission from the two companion galaxies is in agreement with our current understanding of the typical Mid-IR signature in galaxies (Vigroux 1997). In early type galaxies the Mid-IR emission is dominated by the old stellar population. The LW2 flux is typically 6 times stronger than the LW3 emission which is consistent with temperatures of ~5000 K (Madden 1997). Since the LW2 emission of G2 is just ~4 times stronger than the rms noise of the LW3

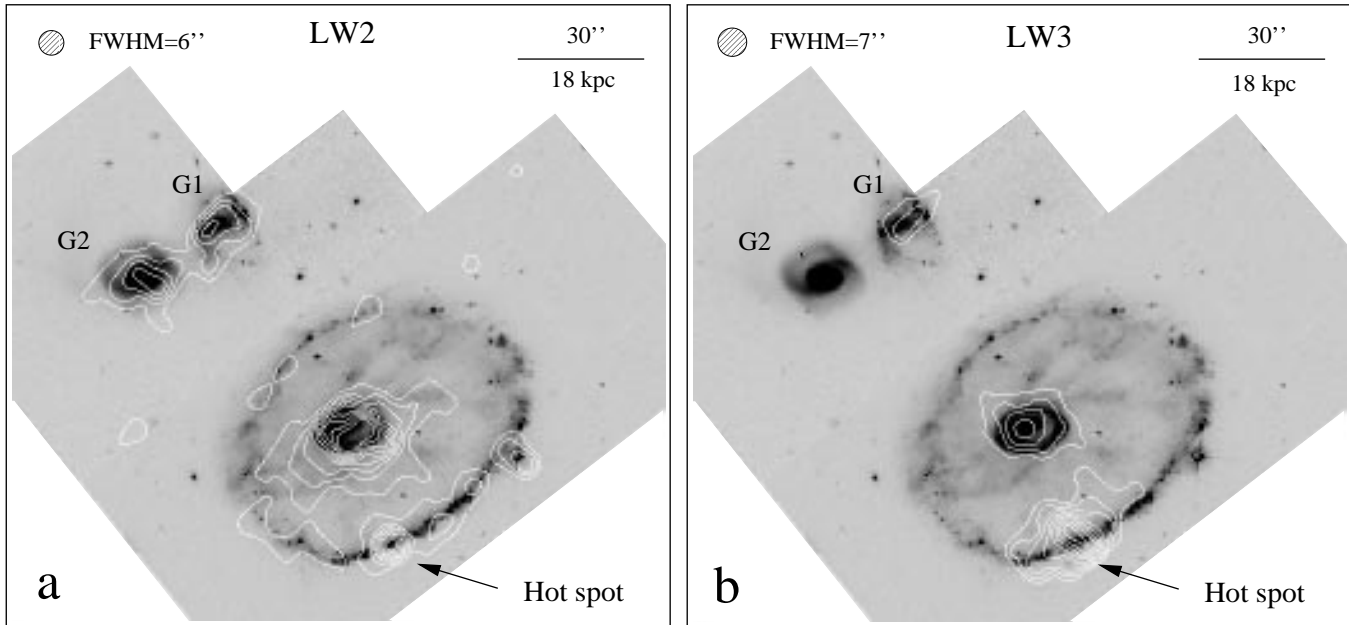


Fig. 1. **a** Contour map of the ISOCAM LW2 emission overlaid on an HST wide I band image. The contour levels are from 0.1 to 0.5 mJy/pixel with a step of 0.05 mJy/pixel. **b** Contour map of the ISOCAM LW3 emission overlaid on the same HST image. The contour levels are 0.2, 0.3, 0.4, 0.6, 0.8, 1, 1.2 and 1.4 mJy/pixel. North is up and East is left in both images.

emission any expected stellar contribution to the LW3 filter measurement would be below our detection limit. The ratio of LW3 to LW2 flux of G1 is ~ 1.4 , a value found in most normal late type galaxies.

3.2. The Cartwheel outer ring

Our ISOCAM observations reveal that one-third of the circumference of Cartwheel's outer ring is detected in the LW2 band (see Fig. 1a). The detected segment of the ring corresponds to the brightest part of the optical ring as defined by the $H\alpha$ image of Higdon (1995). More than 80% of the total $H\alpha$ flux from the Cartwheel outer ring originates from its south-eastern segment. About 60% of the LW2 flux from the outer ring comes from a hot-spot in the ring, unresolved to our observations, which corresponds to the position of two large $H\text{ II}$ region complexes (Higdon 1995).

Interestingly, in the LW3 filter, only the hot-spot is detected in the outer ring (Fig. 1b), and the only other emission from the Cartwheel is from the central regions (see Table 2 and discussion below). The LW3/LW2 flux ratio, often used as a diagnostic of the intensity of the radiation field, of the hot-spot is 5.2, a value which is among the highest detected in all interacting galaxies of the CAMACTIV sample. For comparison, the highest LW3/LW2 flux ratio detected in the interacting galaxy NGC 4038/39 is only 2.6 and it is found in the region where the two disks overlap (Vigroux et al. 1996; Mirabel et al. 1998).

The lack of detection in the LW3 filter from regions of the ring other than the hot-spot is intriguing. What is clear is that if the rest of the ring had the same ratio of LW3/LW2 (i.e. 5.2) as the hot-spot, then it would have been easily detected in the

LW3 band. Therefore, using the rms noise of the LW3 image, as well as the total LW2 flux of the ring (excluding the hot-spot – see Table 2), we set a 2σ upper limit on the LW3 to LW2 ratio of 1.45 in the optically bright regions away from the hot-spot. What could be responsible for the difference in flux ratio for the hot-spot, as compared with the other ring regions?

A clue as to why the hot-spot is different comes from a comparison with radio and optical observations. The hot-spot coincides with the peak of the 20cm and 6cm radio continuum emission from the ring, and, unlike the rest of the outer ring, shows a sudden drop in $H\text{ I}$ surface density at that point (Higdon 1996). Assuming that $H\text{ I}$ absorption is not responsible for the drop in $H\text{ I}$ surface density, then this suggests that most of the cool gas in the hot-spot region is either ionized and/or has already been converted into stars. The very powerful UV radiation field in the hot-spot implied by its radio and $H\alpha$ emission – the $H\alpha$ surface density is at least a factor of 3 times higher there compared with the other regions of the ring (Higdon 1995) – would be expected to illuminate a larger volume of interstellar grains, thereby boosting the thermal continuum at longer wavelengths sampled by the LW3 filter relative to the shorter wavelength PAH-dominated LW2 emission. For an idealized spherical $H\text{ II}$ region of radius R , its volume is proportional to R^3 while the volume of the associated photo-dissociation-region (PDR) which has a shell shape would vary as R^2 . Hence, the filling factor of the $H\text{ II}$ regions in a given giant molecular cloud of the ISM would increase with a higher rate than the corresponding PDRs. Moreover, in a strong UV environment, the dissociation of PAH molecules would further diminish their contribution to the LW2 flux (i.e. Vigroux 1996). These factors can provide a simple explanation for the larger-than-normal ratio

Table 2. Mid-infrared photometry of the Cartwheel group

Region	Area arcsec ²	LW2 mJy	LW3 mJy	$\frac{LW3}{LW2}$
Nucleus	432	3.6 ± 0.14	3.8 ± 0.38	1.1
Hot Spot	324	1.4 ± 0.12	7.5 ± 0.33	5.2
Ring (total)	540	2.3 ± 0.16	8.9 ± 0.43	(3.8)
Cartwheel	972	5.9 ± 0.21	12.7 ± 0.57	(2.2)
G1	324	1.3 ± 0.12	1.9 ± 0.33	1.4
G2	324	1.6 ± 0.12	< 0.3	< 0.2
RMS/pixel		0.04	0.11	

of LW3/LW2 in the hot-spot region based purely on a difference in the strength of the local radiation field.

An explanation for the variable ratio of LW3/LW2 fluxes in the ring may be a purely geometrical one. It is likely that the very strong star formation in the south-western segment of the ring is sufficient to create local galactic fountains which would lift dust grains to large vertical disk scale-heights, the typical size of which can be calculated (i.e. Tenorio-Tagle & Bodenheimer (1988). Based on the 20cm radio continuum flux the type II supernova (SN) rate on the outer ring is $\mu_{SN} = 0.1 \text{ yr}^{-1}$ (Higdon 1996). Since the density wave is propagating with $\sim 40 \text{ km s}^{-1}$ across the disk, for an instantaneous burst model the total number of supernovae created on the outer ring of the Cartwheel ($\sim 5 \text{ kpc}$ in width) is $\sim 10^7$ over a period of 1.2×10^8 yrs. Assuming a typical energy output per supernova of 10^{51} ergs, an ISM density of 1 cm^{-3} , and that the SN are uniformly distributed on the ring, we estimate a vertical scale up to $\sim 4 \text{ kpc}$ (see Tenorio-Tagle & Bodenheimer 1988, Sect. 3.1.1). The previous calculations, though rough, since they do not consider the finite thickness of the galaxy disk, clearly suggest that the gas/dust of the ring will be distributed in a torus-like shape.

This “puffing” of the ring in combination with the stellar winds of the forming stars would result in making the star forming regions density bounded and diluting of the UV field in the local ISM. As distance from the H II regions increases vertically, the heating flux would be lowered, and the small grain emission (and as a result the LW3 flux) would decrease exponentially. On the other hand, since the LW2 band is dominated by thermally-spiked PAH features, its emission strength would decrease almost linearly to the heating intensity (Sauvage et al. 1996), making LW2 stronger relatively to LW3. This could also explain why even though more than 95% of the detected star formation is clearly taking place in the outer ring of the Cartwheel (Amram et al. 1998) the Mid-IR fluxes of the outer ring and nuclear regions are comparable.

3.3. The inner ring and nucleus

Until recently, it was believed that the outer ring of the Cartwheel was the only one that showed signs of star formation activity (Fosbury & Hawarden 1977; Higdon 1995). However, our new observations show conclusively that the inner ring is strongly

detected with ISOCAM. The low spatial resolution of our images does not allow us to resolve the inner ring and dust lanes observed by HST around the nucleus of the Cartwheel (Struck et al. 1996). Although centrally concentrated, the emission from the central regions is resolved and a faint filament of LW2 emission extending to the west of the nucleus follows one of the “spokes” seen in the optical images. However, it was initially a surprise for us to detect such a strong signal from the center of the Cartwheel, which had previously been believed to be almost devoid of nuclear activity (Fosbury & Hawarden 1977, Higdon 1995). The center of the Cartwheel exceeds the outer star-forming ring by a factor of 1.6 in the LW2 filter while it has 0.4 times the flux of the outer ring in the LW3 filter. The nuclear region has Mid-IR colours similar to those of late type galaxies ($LW3/LW2 = 1.1$, see Table 2), although optically, it has very red colours suggestive of an older stellar population (Struck et al. 1996).

We have mentioned that Amram et al. (1998) have recently detected low-level H α emission from the Cartwheel center, a result confirming other independent observations (Higdon priv. comm.). If one assumes that the H α emission originates in normal H II regions, could the observed LW3 emission be explained in terms of warm dust heated by young stars? We can estimate the amount of LW3 flux produced by star formation in the nucleus if we use the LW3 to H α correlation found in M51 (Sauvage et al. 1996). Supposing that the H α flux detected by Amram et al. (1998, see Fig. 1), is distributed over the inner ring annulus (area $\sim 170 \text{ arcsec}^2$) of the Cartwheel and that typically $LW3/H\alpha \sim 30$, we find that *the predicted LW3 is about 3.5 mJy*, which is of the same order as the observed LW3 emission from the Cartwheel center. Hence, it appears that despite its rather low-intensity, star formation activity from the Cartwheel center is sufficient to heat the dust and produce the observed Mid-IR emission.

Another possible source of dust heating in the nuclear region could be attributed to the infall of gas clouds. This was proposed by Struck et al. (1996) based on the morphology of kiloparsec size, cometary-like structures with blue luminosities in the range $1.1\text{--}1.7 \times 10^{40} \text{ ergs s}^{-1}$, detected in the edge of the inner ring. An order of magnitude calculation by the authors suggests that the dissipation of the kinetic energy of the accreting clouds via shocks, would be $\sim 10^{40} \text{ ergs s}^{-1}$, sufficient to generate a fraction of the observed blue luminosities.

4. Conclusions

We have obtained Mid-IR ISOCAM broad-band images of the Cartwheel group and comparing our data with our sample of normal and active galaxies we were able to draw the following conclusions:

- 1) A large segment of the outer ring is detected in the LW2 filter which is mainly dominated by thermally-spiked PAH emission bands, while at longer wavelengths (LW3 filter), where the emission is primarily due to dust grains in nearly thermal equilibrium, the main source of emission originates from a single hot-spot in the ring associated with a particularly bright complex of H II

regions. The hot-spot has an exceptional Mid-IR broad-band diagnostic ratio LW3/LW2 of 5.2 which is among the highest of any region in the CAMACTIV sample and is different from other regions of the ring.

2) A large fraction of the Mid-IR emission is associated with the inner ring and nucleus of the Cartwheel, in stark contrast to that expected from optical emission-line studies (where most of the line emission originates from the outer ring). Recently faint $H\alpha$ emission has been detected from the inner ring and it is possible that this may be due to a low-level star formation which heats the grains. However, in order to explain why the nuclear emission is so powerful compared with the outer ring at ISOCAM wavelengths, it seems that the dust of the outer ring must be spatially distributed very differently. One possibility is that the grains in the outer ring experience a significantly diluted UV radiation field because they are lifted out of the disk by stronger stellar winds. Alternatively, the nuclear regions may be heated by a very different process than the outer, for example shock waves from infalling clouds (Struck et al 1996).

3) The Mid-IR emission from the two companions is typical for their Hubble type.

Even though our observations shed some more light to the properties of the hot dust in the Cartwheel galaxy, the amount and spatial distribution of the cold dust remain uncertain. The 100 μm IRAS flux of the galaxy is 1.6 Jy but previous efforts to detect CO emission (Horellou 1995) were unsuccessful, setting an upper limit to the H_2 mass of $1.5 \cdot 10^9 M_{\odot}$. Could this be explained by the low metallicity of the system, by its intrinsically low molecular gas content or simply by the large distance of the Cartwheel? Where is the peak of the spectral energy distribution in this galaxy? Deep sub-mm and mm wave observations which are scheduled in the near future should enable us to address these questions.

Acknowledgements. The authors are grateful to F. Combes (Obs. de Paris), C. Struck (Iowa State Univ.), C. Horellou (Onsala Space Obs.), and J. Higdon (Kapteyn Institute) for comments and stimulating discussions, as well as the referee for useful suggestions which improved this paper. VC would like to acknowledge the financial support from the TMR fellowship grant ERBFMBICT960967 and the help of all members of the ISOCAM team at CEA-Saclay.

References

- Abergel A., Bernard J.P., Boulanger F., et al., 1996, A&A 315, L329
 Amram P., Mendes de Oliveira C., Boulesteix J., Balkowski C., 1998, A&A 330, 881
 Appleton P.N., 1998, In: Barnes J., Sanders D. (eds.) Galaxy Interactions at Low and High Redshift. IAU 186, in press
 Appleton P.N., Marston A.P., 1997, AJ 113, 201
 Appleton P.N., Struck-Marcell C., 1987, ApJ 312, 103
 Appleton P.N., Struck-Marcell C., 1996, Fund. of Cos. Phys. 16, 111
 Biviano A., Sauvage M., Roman P., E.S.A/C.E.A Technical Report, December 1997
 Borne K.D., Appleton P.N., Lucas R.A., Struck C., Schultz A.B., 1997, Rev. Mex. Astron. Astrofis. 6, 141
 Cesarsky C.J., Abergel A., Agnèsè P., et al., 1996, A&A 315, L32
 Davies R., Morton D., 1982, MNRAS 201, 69
 Delaney M., 1997, ISOCAM Interactive Analysis User's Manual. SAI-96-5226/Dc.
 Fosbury R., Hawarden T., 1977, MNRAS 178, 473
 Hernquist L., Weil M., 1993, MNRAS 261, 804
 Higdon J., 1995, ApJ 455, 524
 Higdon J., 1996, ApJ 467, 241
 Horellou C., Casoli F., Combes F., Dupraz C., 1995, A&A 298, 743
 Kessler M.F., Steinz J.A., Anderegg, M.E., et al., 1996, A&A 315, L27
 Lynds R., Toomre A., 1976, ApJ 209, 382
 Madden S., 1997, In: Mamon G.A., Trinh Xuan Thuan, Tran Thanh J. (eds.) XVIIth Moriond Astrophysics Meeting: Extragalactic Astronomy in the Infrared. p. 229,
 Marcum P., Appleton P.N., Higdon J., 1992, ApJ 399, 57
 Mirabel I.F., Vigroux L., Charmandaris V., et al., 1998, A&A 333, L1
 Sauvage M., Blommaert J., Boulanger F., et al., 1996, A&A 315, L89
 Starck J.-L., Claret A., Siebenmorgan R., C.E.A. Technical Report, March 1996
 Starck J.-L., Abergel A., Aussel H., et al., 1998, A&AS 133, in press
 Struck C., 1997, ApJS 113, 269
 Struck C., Appleton P.N., Borne K.D., Lucas R.A., 1996, AJ 112, 1868
 Struck-Marcell C., Higdon J., 1993, ApJ 411, 108
 Tenorio-Tagle G., Bodenheimer P., 1988, ARA&A 26, 145
 Theys J., Spiegel E., 1976, ApJ 212, 616
 Vigroux L. 1997, In: Mamon G.A., Trinh Xuan Thuan, Tran Thanh J. (eds.) XVIIth Moriond Astrophysics Meeting: Extragalactic Astronomy in the Infrared. p. 63
 Vigroux L., Mirabel I.F., Altieri B., et al., 1996, A&A 315, L93
 Zwicky F., 1941, In: Contribution to Applied Mechanics and Related Subjects. Theodore von Karman Anniversary volume, California Institute of Technology, Pasadena, California, p. 137